Invisible grazings and dangerous bifurcations in impacting systems: The problem of narrow-band chaos

Soumitro Banerjee,[1] James Ing,[2] Ekaterina Pavlovskaia,[2] Marian Wiercigroch,[2] and Ramesh K. Reddy[1]
[1]*Department of Electrical Engineering, Indian Institute of Technology, Kharagpur 721302, India*
[2]*Centre for Applied Dynamics Research, School of Engineering, University of Aberdeen, Kings College, Aberdeen Ab24 3UE, United Kingdom*
(Received 6 November 2008; published 17 March 2009)

We discovered a narrow band of chaos close to the grazing condition for a simple soft impact oscillator. The phenomenon was observed experimentally for a range of system parameters. Through numerical stability analysis, we argue that this abrupt onset to chaos is caused by a *dangerous bifurcation* in which two unstable period-3 orbits, created at "invisible" grazings, take part.

DOI: 10.1103/PhysRevE.79.037201 PACS number(s): 05.45.Ac

Physical systems undergoing intermittent contact with a relatively rigid barrier are ubiquitous, since gaps can arise through wear, limited tolerances in manufacture, motion outside of an anticipated regime, or as a design feature. We experimentally demonstrate that such systems may exhibit a peculiar dynamical behavior where the orbit abruptly jumps to a large-amplitude chaotic motion close to a grazing condition, which lasts for a very narrow range of the parameter. We show that this phenomenon is caused by two unstable periodic orbits, born at a different parameter value, which remain unobserved until they precipitate a *dangerous bifurcation* [1], causing the abrupt divergence of the orbit.

Many differing approaches exist to model impacting motion, and this is further complicated by the relative sparsity of experiments. The archetype of impacting systems is a bilinear oscillator where the stiffness takes two distinct values. When the ratio of these is high the contact can be well approximated by a rigid stop [2]. We undertook a systematic investigation of such a system using an experimental impacting system built in the University of Aberdeen, U.K., and shown in Fig. 1. It is a vertically aligned mass-spring-damper system with sinusoidal base excitation, and the mass can impact upon a small bolt supported by another spring. The full details of the experimental rig and measuring procedures can be found in [3]. Experimental bifurcation diagrams were constructed in the following way. First the nonimpacting linear response was established for sufficiently low excitation frequency. The frequency was then incrementally increased through the grazing conditions of the linear response and beyond. For each chosen set of parameters a steady-state response was reached prior to data capture. Next, a first return Poincaré map was constructed and projected onto the displacement axis. The Poincaré plane was placed at various phases (constant for each bifurcation diagram) in order to maximize the separation between the points appearing on the diagram.

The results were obtained for a natural frequency of 9.38 Hz, a gap of 1.26 mm, a damping coefficient of 1.3 kg/s and secondary spring stiffness 29 times higher than that of the main one. Bifurcation scenarios near grazing observed experimentally for excitation amplitude equal to 0.44, 0.66, and 0.70 mm are shown in Fig. 2. It is found that under different parameter regimes the border collision bifurcation can result in a transition from the nonimpacting period-1 orbit to an impacting period-2 orbit [Fig. 2(a)], an impacting period-3 orbit [Fig. 2(b)], or an impacting period-1 orbit [Fig. 2(c)]. But in all these cases there is a narrow band of chaos close to the grazing condition. This is observed for a variety of parameters and seems to be in some way generic.

The importance of a zero velocity "grazing" impact is well established and manifests differently when the impact is with a rigid or yielding barrier [4,5]. For instantaneous impacts with a rigid stop the derived normal form map contains a square-root term causing a singularity in the first derivative and a corresponding stretching in one eigendirection. This causes an abrupt loss in the stability, since at grazing one of the eigenvalues jumps outside of the unit circle. In the case of impact with an elastically yielding barrier the resulting normal form map contains a 3/2 term (to lowest order) which results in smooth derivatives and continuous eigenvalues. Although it has been shown that the behavior becomes effectively that of a square-root map for higher velocity impacts, there is no loss of stability at the grazing conditions and smooth bifurcations can occur [5].

Thus in hard-impact oscillators, the orbit experiences a high degree of stretching close to the grazing condition ow-

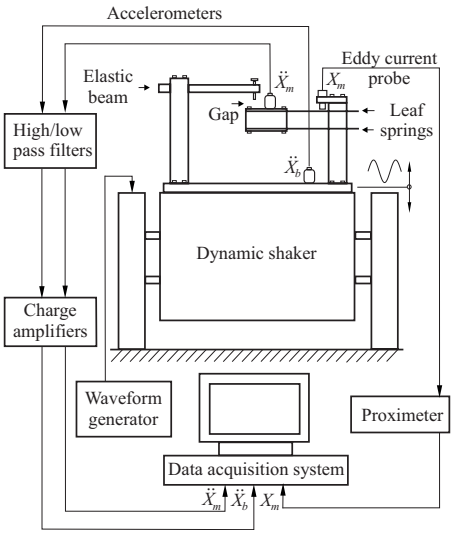

FIG. 1. Schematic diagram of the experimental rig [3].

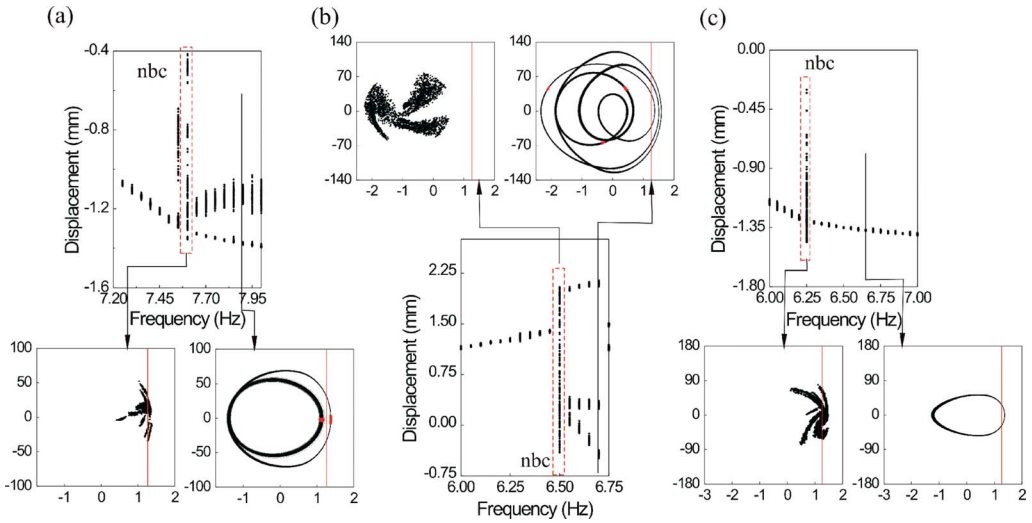

FIG. 2. (Color online) Narrow band of chaos detected on bifurcation diagrams obtained for (a) excitation amplitude equal to 0.44 mm, (b) excitation amplitude equal to 0.66 mm and (c) excitation amplitude equal to 0.70 mm. Additional windows show (a) the chaotic orbit in the Poincaré section at $f=7.60$ Hz and the continuous-line orbit at 7.90 Hz, (b) the discrete-time chaotic orbit at $f=6.50$ Hz and the phase-plane trajectory at 6.70 Hz, and (c) the discrete-time chaotic orbit at $f=6.25$ Hz and phase-plane trajectory at 6.65 Hz. The vertical red lines indicate the switching manifold.

ing to the repeated application of the square-root map [5]. One can expect a divergence away from the local attractor, and the resulting attractor should have a fingered structure comprising of the stretching direction in the Poincaré plane and its forward iterates. In our experimental system, since the spring in the support is much stiffer than the main one, the map starts to demonstrate a similar stretching behavior when the penetration becomes significant. Thus one can expect a sudden expansion of the attractor and the onset of sensitive dependence on initial conditions shortly after the grazing parameter value. This much can be inferred on the basis of current knowledge. We have discovered that something in addition to the above is responsible for the creation of the narrow-band chaos.

Theoretical investigations of the considered oscillator were conducted using the nondimensionalized equations of motion derived in [2,3]

$$x' = v,$$

$$v' = a\omega^2 \sin(\omega\tau) - 2\xi v - x - \beta(x-e)H(x-e), \qquad (1)$$

where $x=y/x_0$ and $v=dx/d\tau$ are nondimensional displacement and velocity of the oscillator, $\tau=2\pi f_n t$ is nondimensional time, $f_n=\frac{1}{2\pi}\sqrt{k_1/m}$ is the natural frequency for the undamped linear system (in Hz), x_0 is some arbitrary reference distance, and $H(\cdot)$ is the Heaviside step function. Here $\beta=k_2/k_1$ is the stiffness ratio, $\omega=f/f_n$ is the frequency, $e=g/x_0$ is the gap, $\xi=c/(4m\pi f_n)$ is the damping ratio, and $a=A/x_0$ is the forcing amplitude—all in nondimensional form.

The bifurcation scenario corresponding to the one shown in Fig. 2(a) was obtained numerically for $\xi=0.01$, $\beta=29$, $e=1.26$, and excitation amplitude $a=0.7$ under varying excitation frequency ω, and it is presented in Fig. 3. Here additional windows showing the chaotic orbit at $\omega=0.8023$ (in the Poincaré plane) and the period-2 orbit at $\omega=0.84$ (in continuous time) demonstrate the good correspondence with the experimental results.

Initially, for a nondimensional excitation amplitude $a=0.7$ and nondimensional frequency $\omega=0.76$, the orbit is nonimpacting. As the parameter ω is increased, the period-1 orbit undergoes grazing at $\omega=0.801\,928$. The grazing frequency is calculated from the relation $a\omega^2=e\sqrt{(1-\omega^2)^2+4\xi^2\omega^2}$, obtained using the exact solution of the nonimpacting system equations.

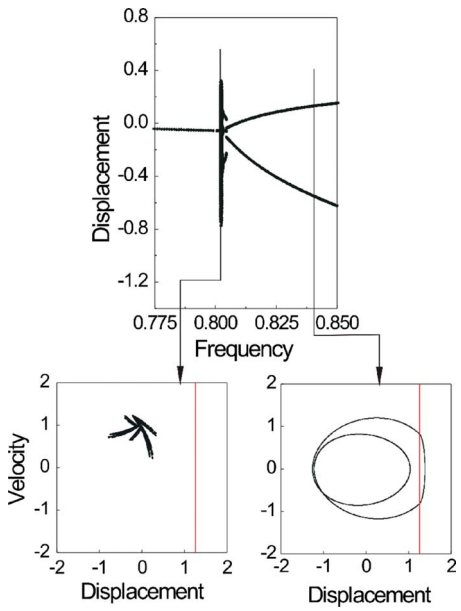

FIG. 3. (Color online) Numerically obtained bifurcation diagram for the mass displacement under varying frequency ω at $\xi=0.01$, $\beta=29$, $e=1.26$, and excitation amplitude $a=0.7$. Additional windows demonstrate the orbits for $\omega=0.8023$ and 0.84, respectively.

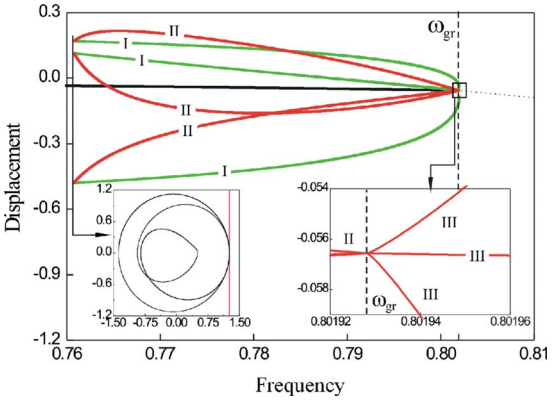

FIG. 4. (Color online) Bifurcation diagram showing the evolution of the period-1 and period-3 orbits for the limiting case of hard-impact system. The stable periodic orbit is denoted by black and the two unstable period-3 orbits by red and green, respectively. Left inset: the period-3 grazing orbit at $\omega_1=0.760\ 761\ 39$. Right inset: close-up of the bifurcation diagram close to the grazing point.

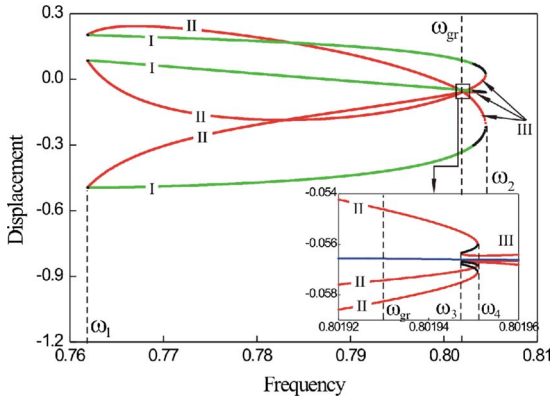

FIG. 5. (Color online) Bifurcation diagram showing the evolution of the period-1 and period-3 orbits in the soft impact system with stiffness ratio 29. The stable period-1 orbit is denoted by blue, stable period-3 orbits by black, and the two unstable period-3 orbits by red and green.

Just before grazing of the nonimpacting linear orbit, the eigenvalues are $0.017\ 821 \pm i0.924\ 468$. Following grazing, the eigenvalues still have modulus less than unity, and so the orbit is stable. However, in the experiment described above, we see the onset of a chaotic orbit at this point. Numerical investigation shows that even though the orbit is stable, a slight perturbation in the initial conditions makes the state diverge from it and form a much larger chaotic orbit. As the parameter is increased further, it is found that the period-1 orbit becomes unstable through a smooth period-doubling bifurcation at $0.802\ 035\ 2$. This results in the creation of a stable period-2 orbit with two impacts. As the parameter is further increased to $\omega=0.802\ 074\ 7$, the period-2 orbit undergoes a boundary crisis induced by grazing. However, all through this narrow range, we see the chaotic orbit.

These observations raise some natural questions. How can the state move away from the periodic orbit that is stable? What forms the chaotic orbit?

To probe this question, we have developed an algorithm that can detect periodic orbits, possibly with multiple impacts, irrespective of their stability through a Newton-Raphson search procedure. In each step the Jacobian matrix is composed of the exponential matrices for the passages through the linear subsystems and saltation matrices for the passages across the switching manifolds. As a parameter is varied, the program can follow periodic orbits—stable or unstable—where the location of the periodic orbit for any parameter value is taken as the initial guess for the next value.

For convenience of explanation, we first analyze the case of hard impact, i.e., when the stiffness ratio tends to infinity. We found that many other high-periodic orbits exist over a parameter range that includes the grazing value, out of which we concentrate on the evolution of the period-3 orbits shown in Fig. 4 which is calculated for $\beta=5000$.

This figure reveals that long before the main period-1 orbit grazes the switching manifold, two period-3 orbits come into existence at $\omega_1=0.760\ 761\ 39$. At the point of birth, the two orbits coincide in a grazing condition (the left inset of Fig. 4). Both the new-born period-3 orbits are unstable, and that is why they are not observed in experiment or in the usual numerical computation of the bifurcation diagram. This grazing did not physically occur but could occur if the appropriate parameters and initial conditions were chosen. We shall call it an "invisible grazing," which exerts significant influence on the dynamics of the system. Note that in a smooth system, pairs of periodic orbits can come into existence through a saddle-node bifurcation, and in that case one of the orbits is stable. But in case of a nonsmooth system, both the nascent periodic orbits can be unstable [6].

As the parameter is varied, at $\omega_{gr}=0.801\ 928$ the period-1 orbit grazes the switching boundary. This results in another border collision bifurcation. At that point a strange event takes place.

The stable manifold of one of the period-3 orbits (marked as II) that was created at the invisible grazing forms the basin boundary of the period-1 orbit. As the parameter approaches the grazing value, the distance between the period-1 orbit and the period-3 orbit reduces, and at the bifurcation point the two orbits converge. As a result, at the bifurcation point the basin of attraction shrinks to zero size. This phenomenon, called dangerous bifurcation [1], has been predicted from theoretical considerations. We have thus found an example of a physical system where a dangerous bifurcation occurs.

In the case of the system under consideration, since the stiffness ratio is high, its behavior closely approximates that of the hard-impact system. But since the wall is now compliant, the map is smooth. This has the effect of smoothening the bifurcations described above (see Fig. 5 calculated for $\beta=29$).

In this case the two period-3 orbits are born at $\omega_1=0.761\ 8806$ via a smooth saddle-node bifurcation close to the point of invisible grazing. The node (branch I) loses stability shortly after—at $\omega=0.761\ 958$ through a period-doubling bifurcation. The other unstable period-3 orbit (branch II) approaches the period-1 orbit as the grazing parameter value $\omega_{gr}=0.801\ 928$ is approached from below. Another unstable period-3 orbit (branch III in Fig. 5), born via a saddle-node bifurcation at ω_2, approaches from above. On a

coarse scale the event at the grazing point looks the same as that in Fig. 4, but the smoothening effect is revealed on close inspection. The close-up of the bifurcation diagram (the inset of Fig. 5) shows two smooth saddle-node bifurcations occurring at very close parameter values, ω_3 and ω_4, connecting unstable branches II and III with a stable period-3 orbit. Close to the grazing parameter value of ω_{gr}, the unstable period-3 orbit that forms the basin boundary comes very close to the periodic orbit. Thus, while in the nonsmooth approximation the distance between the fixed point and the unstable period-3 orbit is ideally zero at the bifurcation point; in the actual system there exists a very small but finite distance. If the ambient noise in the system (which is always present in a realistic situation) can perturb the state across the basin boundary, the state diverges away from the fixed point. Thus, even though the system is smooth in the ultimate analysis, a condition similar to that in dangerous border collision bifurcation is created.

The question is, where does it diverge to? Notice that another unstable period-3 orbit (branch I in Fig. 5) exists at this parameter value. While diverging away from the period-1 fixed point when the state meets the unstable manifold of this period-3 point, the further iterations are constrained to remain on this unstable manifold. Thus, abruptly the unstable manifold of this period-3 fixed point becomes a stable attractor. Figure 6 shows the structural similarity between the unstable manifold of the period-3 saddle point (calculated using the DYNAMICS software [7]) and the chaotic orbit. Note that this narrow-band chaotic orbit was possible due to the existence of the unstable period-3 orbits, which, in turn, was caused by the invisible grazing in the hard-impact case or its smooth approximation in the soft impact case.

The unstable period-3 orbit subsequently becomes stable through a reverse period-doubling bifurcation (see the black portion in Fig. 5). This orbit and the unstable period-3 orbit created at ω_3 merge and disappear at a smooth saddle-node bifurcation at the parameter value ω_2. If the parameter is reduced from this value, the stable period-3 orbit is seen to undergo a smooth period-doubling cascade with periodicities 3, 6, 12, 24, 48, 96, and 192 with a Feigenbaum number of 4.669 201 609…; but then the orbit expands to a larger chaotic orbit. This is caused by an interior crisis, where a point of the periodic orbit touches the stable manifold of the other period-3 saddle.

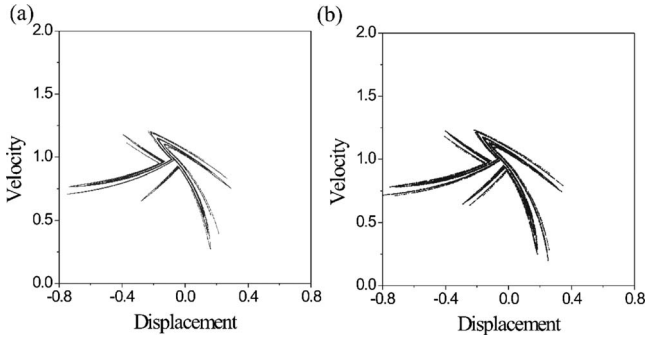

FIG. 6. (a) Unstable manifold for period-3 attractor at $\omega = 0.802$ and (b) chaotic attractor at the same frequency.

Thus the chaotic orbit occurs for the narrow band of parameters from $\omega \approx 0.801\,928$ up to the parameter value of the interior crisis $\omega = 0.802\,645$. Our investigation of the other parameter ranges shows that the above mechanism is a generic one wherever the narrow band of chaos is observed close to grazing in an impacting system and that the occurrence of dangerous bifurcation has to be considered in addition to the stretching behavior predicted by the structure of the Poincaré map to obtain a complete explanation of the observed phenomenon.

J.I. and E.P. would like to acknowledge the financial support from EPSRC under Grant No. EP/E011535.

[1] M. A. Hassouneh, E. H. Abed, and H. E. Nusse, Phys. Rev. Lett. **92**, 070201 (2004); A. Ganguli and S. Banerjee, Phys. Rev. E **71**, 057202 (2005).
[2] S. W. Shaw and P. J. Holmes, J. Sound Vib. **90**, 129 (1983).
[3] J. Ing, E. E. Pavlovskaia, M. Wiercigroch, and S. Banerjee, Philos. Trans. R. Soc. London, Ser. A **366**, 1866 (2008); M. Wiercigroch and V. W. T. Sin, ASME J. Appl. Mech. **65**, 657 (1998).
[4] A. B. Nordmark, J. Sound Vib. **145**, 279 (1991); H. Dankowicz and A. B. Nordmark, Physica **136D**, 280 (2000); J. Molenaar, J. G. de Weger, and W. van de Water, Nonlinearity **14**, 301 (2001); P. Thota and H. Dankowicz, Physica D **214**, 187 (2006).
[5] M. di Bernardo, C. J. Budd, A. R. Champneys, and P. Kowalczyk, *Piecewise-smooth Dynamical Systems: Theory and Applications* (Springer-Verlag, New York, 2008).
[6] S. Banerjee and C. Grebogi, Phys. Rev. E **59**, 4052 (1999).
[7] H. E. Nusse and J. A. Yorke, *Dynamics: Numerical Explorations* (Springer-Verlag, New York, 1998).